Beam Physics Note
TRI-BN-23-13
May 30, 2023

ISAC RF Booster Insertion Optics

Olivier Shelbaya, Rick Baartman

TRIUMF

Abstract: This report presents a new electrostatic quadrupole optics to accommodate ISAC-RFQ beam injection while also producing a round waist inside the triple-gap RF booster cavity, located upstream of the RFQ.

Contents

1 Introduction

This note presents a new beam optics necessary to accommodate the triple-gap rf booster cavity[1], located upstream of the ISAC-RFQ and downstream of the prebuncher[2]. Two principal applications of the new triple gap structure are presented, including space charge compensation in which the longitudinal bunch length is corrected with the cavity, in addition to injected RFQ beam energy compensation. This does not claim to show an exhaustive study of the booster-RFQ relationship, but rather to demonstrate the feasibility of the new RFQ injection optics design.

2 Lattice Concept

This section presents the periodic lattice as originally devised in TRANSOPTR*. For the final dimensions, see Section 5.* The basic structure consists of three quadrupoles, mirrored and repeated three times-over. Figure 1 shows beamspot imaging from the RF booster midpoint to RFQ injection, using six quadrupoles mirrored about the mid-point of the plot. By design, the tune is computed to produce $r_{12} = r_{34} = 0$ at the symmetry point (Fig. 1, *SYM*), while producing $\mathbf{M}_{21} = \mathbf{M}_{43} = 0$ from end-to-end. Tying the quadrupoles together will keep the number of adjustable setpoints minimal.

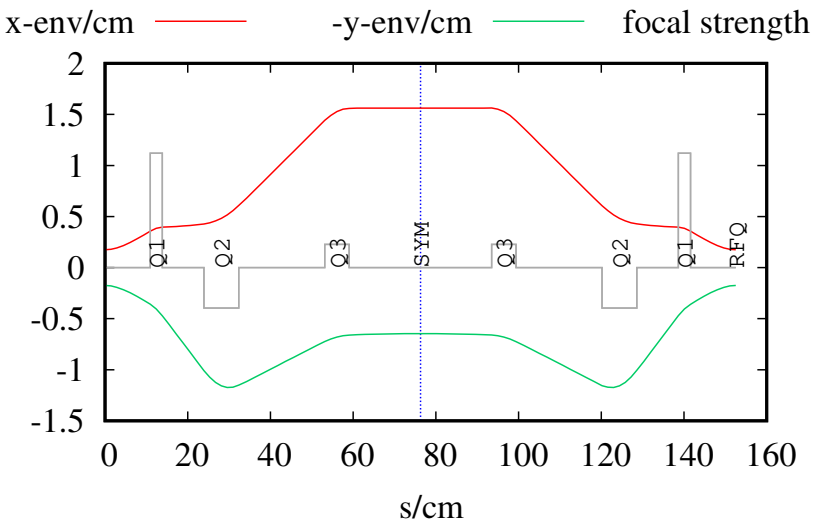

Figure 1: TRANSOPTR computed (x, y) envelopes showing a focus-to-focus, starting at the RF booster midpoint and terminating at RFQ injection. Quadrupole relative focal strengths are shown in grey. Symmetry point *SYM* delineated with dotted blue line.

Figure 2 shows envelopes from the ISAC prebuncher[3] to ISAC-RFQ injection, zeroing $\mathbf{M}_{21}$ and $\mathbf{M}_{43}$. For reference, the original optics' tune is shown as dotted lines. Injection and acceleration in the ISAC-RFQ[4, 5] is shown in Figure 3, with the simulation ending at the rough location of the

chopperslit[6]. In Figure 5, the booster cavity corrects the beam E/A from 1.7 keV/u to 2.04 keV/u. The new optics maintain the ability to inject beam into the RFQ. Since beam energy can change downstream of the booster, the first three new quadrupoles are independently powered from the last six. Figure 4 shows the RF booster enabled, with a bunch charge of 5×10^{-13}C, in which the space

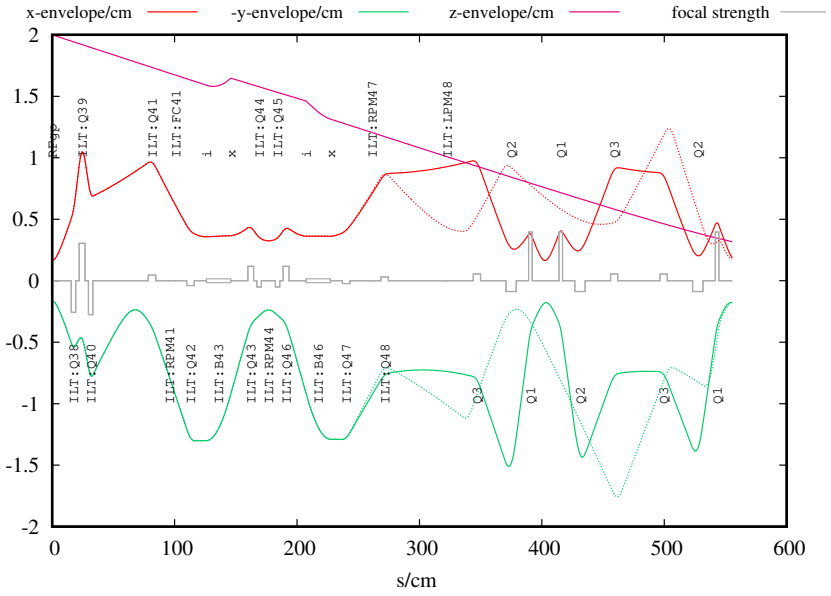

Figure 2: `TRANSOPTR` (x, y) envelopes showing a focus-to-focus, starting at the ISAC prebuncher midpoint and terminating at RFQ injection. Quadrupole relative focal strengths are shown in grey. Symmetry point *SYM* delineated with dotted blue line. An emittance of 50μm is used.

charge self-force causes degradation of the longitudinal time-focus induced by the prebuncher. The booster has been used to re-establish a time-focus at RFQ injection.

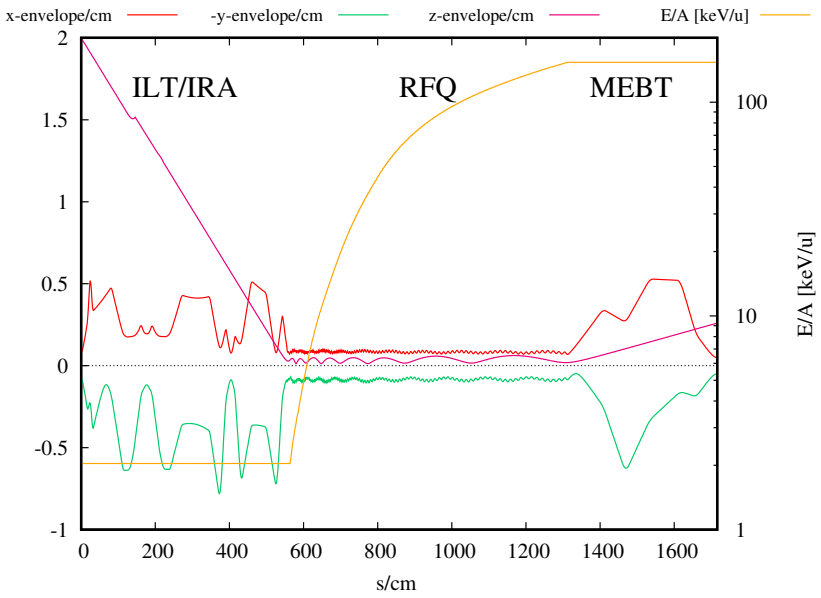

Figure 3: TRANSOPTR (x, y) envelopes showing transport from prebuncher-focus to MEBT:RPM5, including RFQ acceleration to $E/A = 153$ keV/u, up to the MEBT chopperslit. An emittance of 50μm is used.

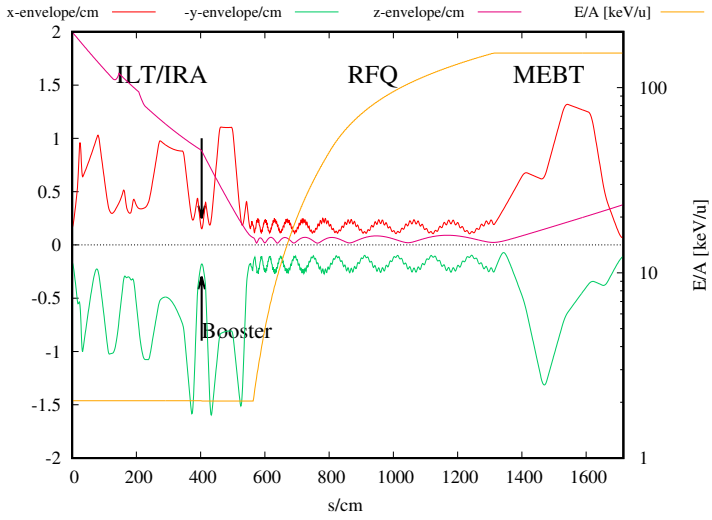

Figure 4: TRANSOPTR (x, y) envelopes showing transport from prebuncher-focus to MEBT:RPM5, including RFQ acceleration to $E/A = 153$ keV/u and RF booster compensation, up to the MEBT chopperslit. An emittance of 50μm is used.

3 CANREB Tie-In: Adjusting Dimensions

The RFQ injection line will intersect a beamline from the CANREB section, shown in Figure 6. The original optics are shown in Figure 7. The location of the cross with respect to the new optics is shown in Fig. 8, with the CANREB line as the horizontal blue lines, showing the centerpoint and 15 cm width of the vacuum line. The new RFQ optics originally placed a Q3 type quadrupole, of effective length 5.89 cm, near to the CANREB-to-ISAC beamline. This creates an asymmetric transverse constraint, which allows for an unobstructed circle of radius 3.08 cm to be centered on the beam axis, shown in Figure 9. This would have limited CANREB envelopes must be kept below this radius for full transmission. This may also cause a steering sensitivity to transmission, if beam from CANREB is slightly off axis. Additionally, the physical length of the quadrupole including skimmer plates will exceed the effective length, increasing the constraint.

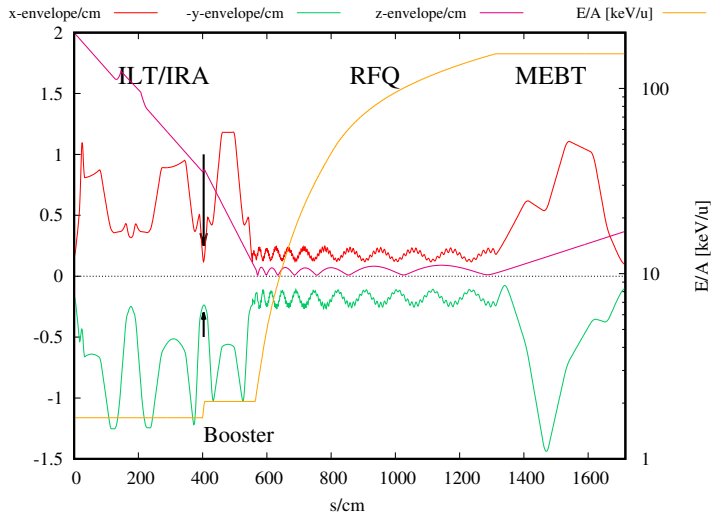

Figure 5: `TRANSOPTR` (x, y) envelopes showing rf booster RFQ injection energy compensation, from prebuncher-focus to MEBT:RPM5, including RFQ acceleration to $E/A = 153$ keV/u, up to the MEBT choppersslit. An emittance of 50μm is used. Since the beam energy changes across the booster, the second and third period (quadrupoles downstream of the booster) are decoupled from the three new quadrupoles upstream of the booster.

To resolve this issue, the quadrupole q3 in the period is moved 5cm away from the symmetry point, effectively extending the q3-q3 drift by 10cm in Figure 1. The envelopes produced by this modification are shown in Figure 10 and the layout with CANREB line in Fig. 11. The first three quadrupoles downstream of ILT:Q48 are independently driven, with the second and third period quadrupoles tied-in together. This produces a six parameter optimization which is easily handled by `TRANSOPTR` and provides flexibility for interoperability with the upstream bend section.

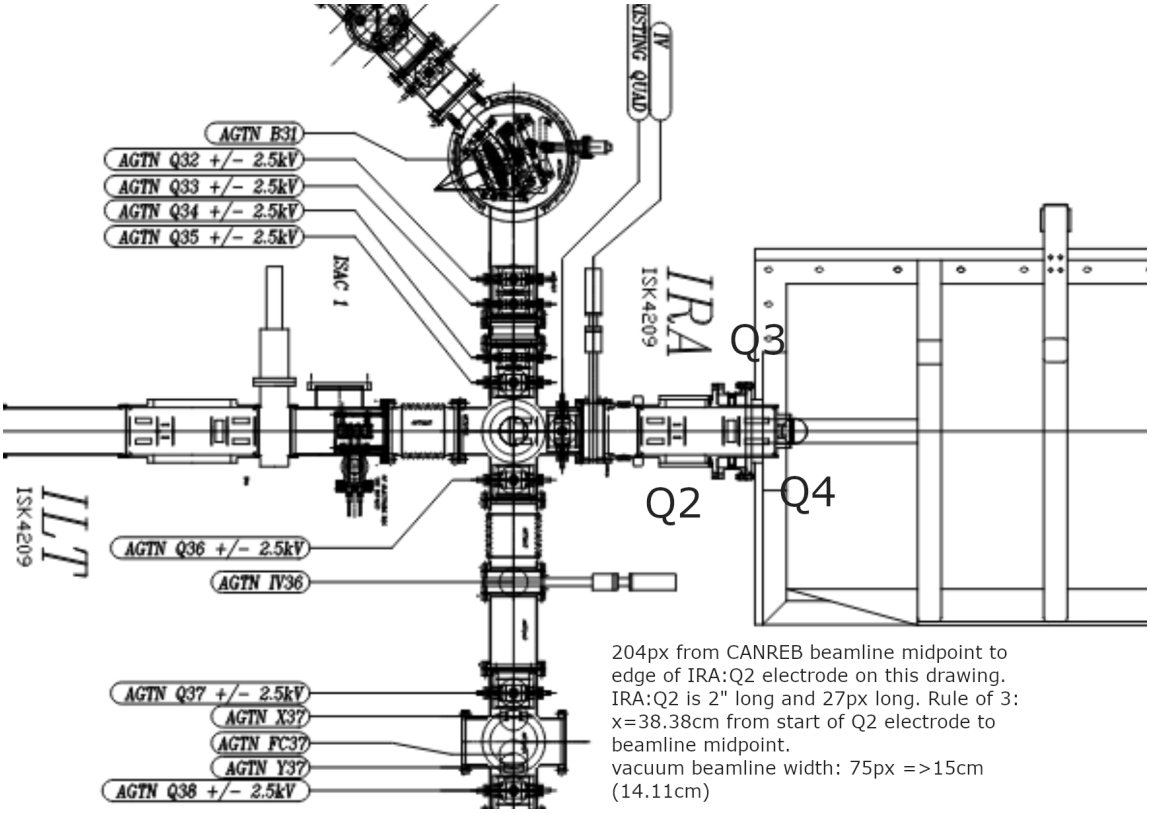

Figure 6: Annotated rendering of CANREB-IRA cross, used for beamline overlap estimation. This drawing and the known electrode length for IRA:Q2 (2”) has been used to estimate the location of the cross with respect to the new injection optics.

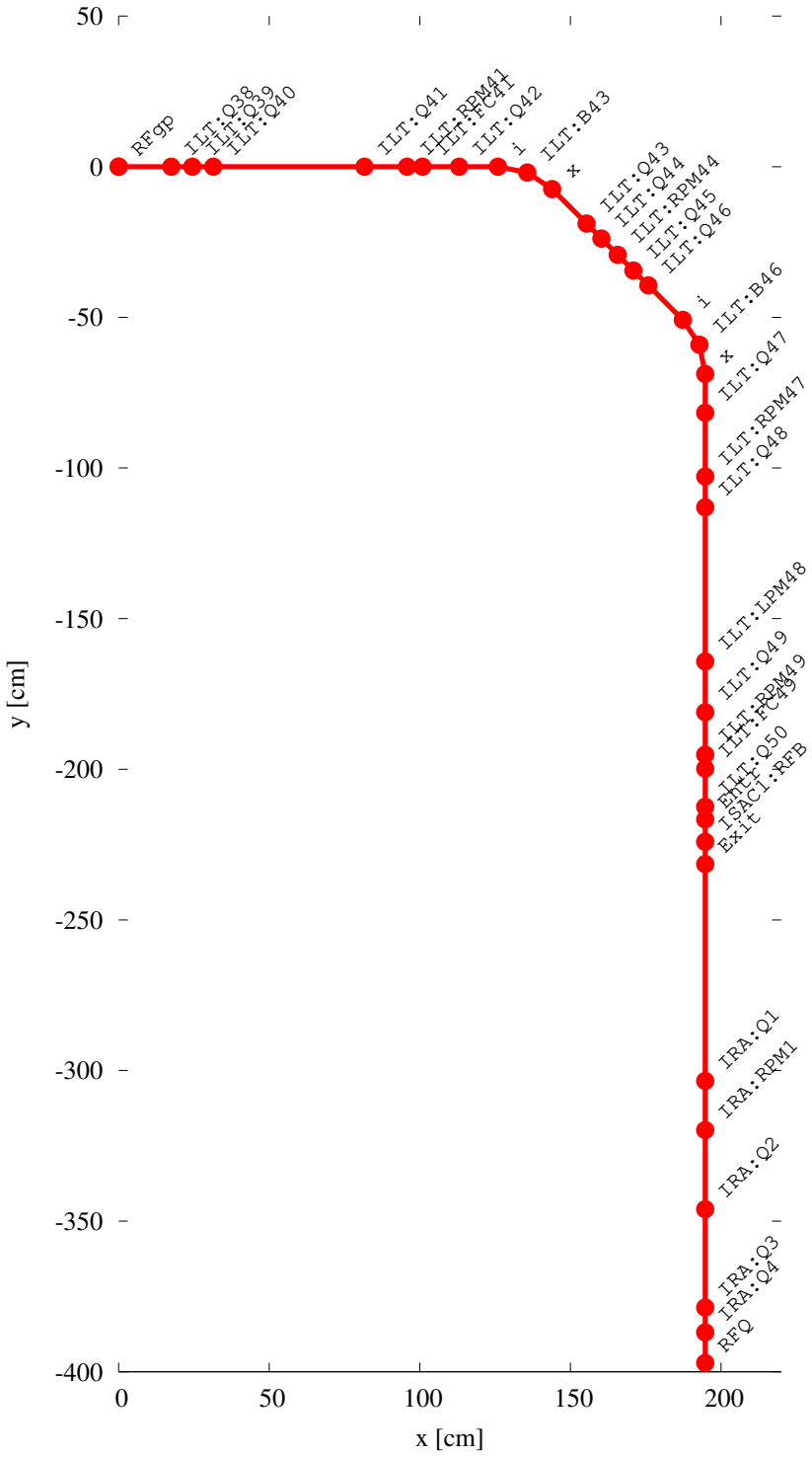

Figure 7: Original ILT/IRA beamline layout, for reference. Beam propagates clockwise from top left to bottom right.

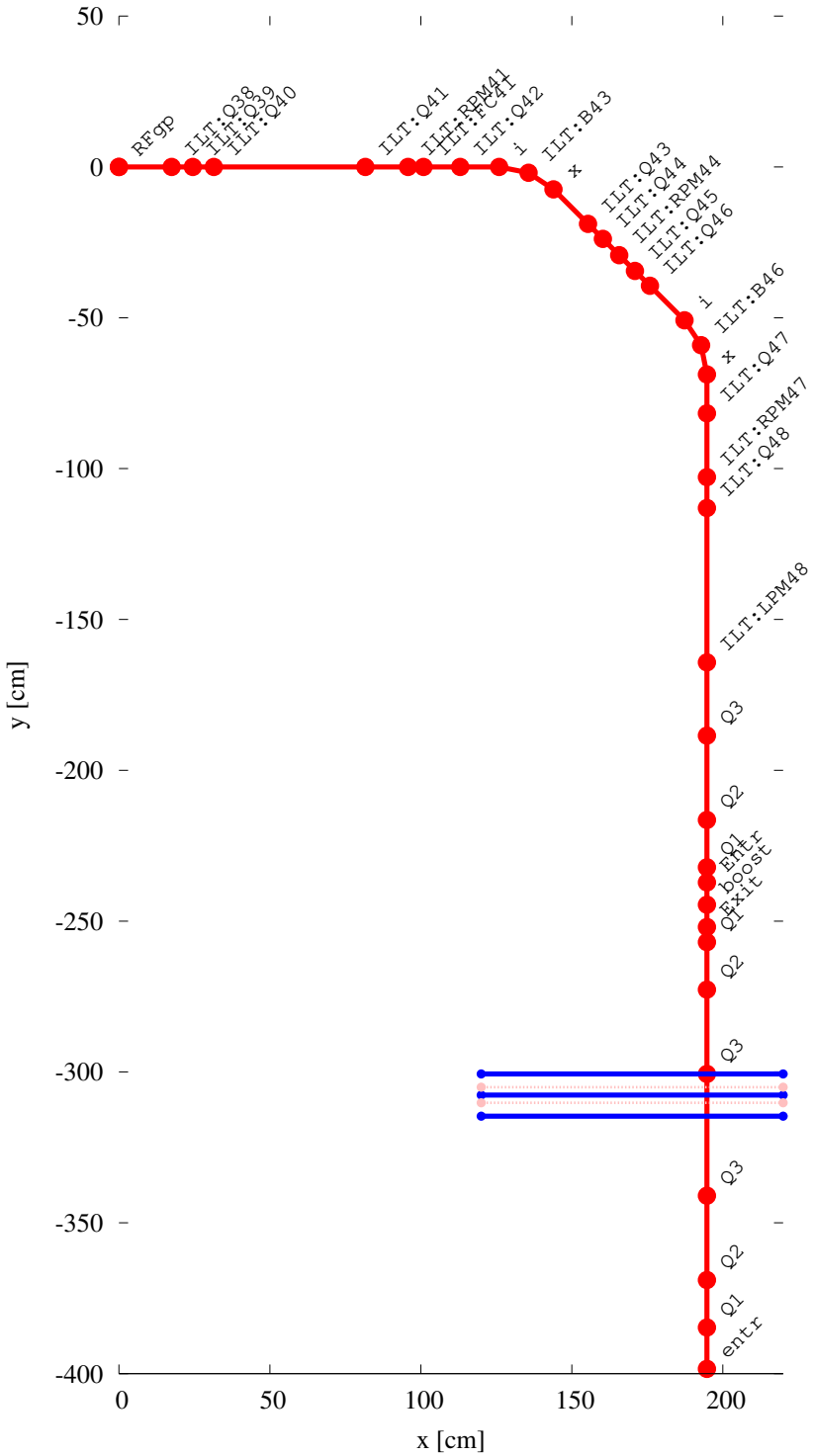

Figure 8: New ILT/IRA beamline layout, **with original Q3 positions**. Beam propagates clockwise from top left to bottom right. Blue horizontal lines show width of CANREB vacuum beamline at location of cross, shown in Figure 6. The new quadrupole Q3, of effective length 5.89 cm, is expected to create a half-aperture constraint allowing for a maximum 6 cm round beamspot at the cross. Since this exceeds any likely beamsize for CANREB to ISAC tunes, it should produce no obstruction to beam transport.

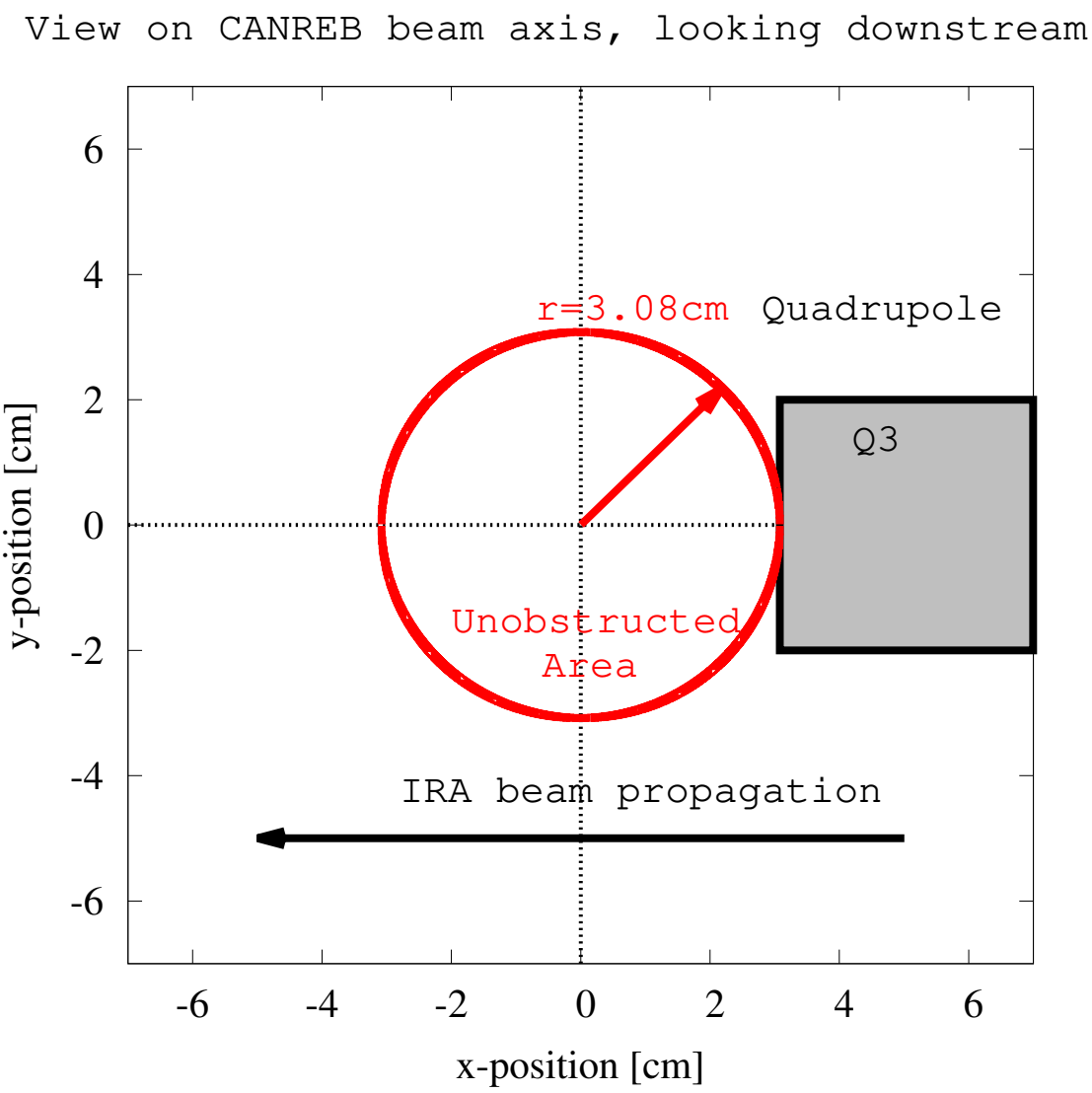

Figure 9: Cross sectional representation, viewed from the CANREB line and looking downstream, at the location of the cross.

4 Steering and Diagnostics

A reverse-progatation model of the injection optics is built and shown in Figure 12, using the tune from Figure 10. The reference particle has been started with a 1 cm offset but no transverse momentum, showing the transverse kicks received by the quadrupoles. For a steerer to have a meaningful effect, the impulse should be given where nontrivial position-momentum correlations exist, in other words where the centroid exhibits a slope. Note that the original ILT/IRA optics for this segment makes use of two sets of $(x, y,)$ steerers, for reference. In Fig. 12, free areas which are potentially suitable to receive a steerer assembly are highlighted in grey along with the approximate clearance area along the optical axis. This, together with the reference particle's centroid location allows for the identification of four locations where (x, y) corrective steering can be located.

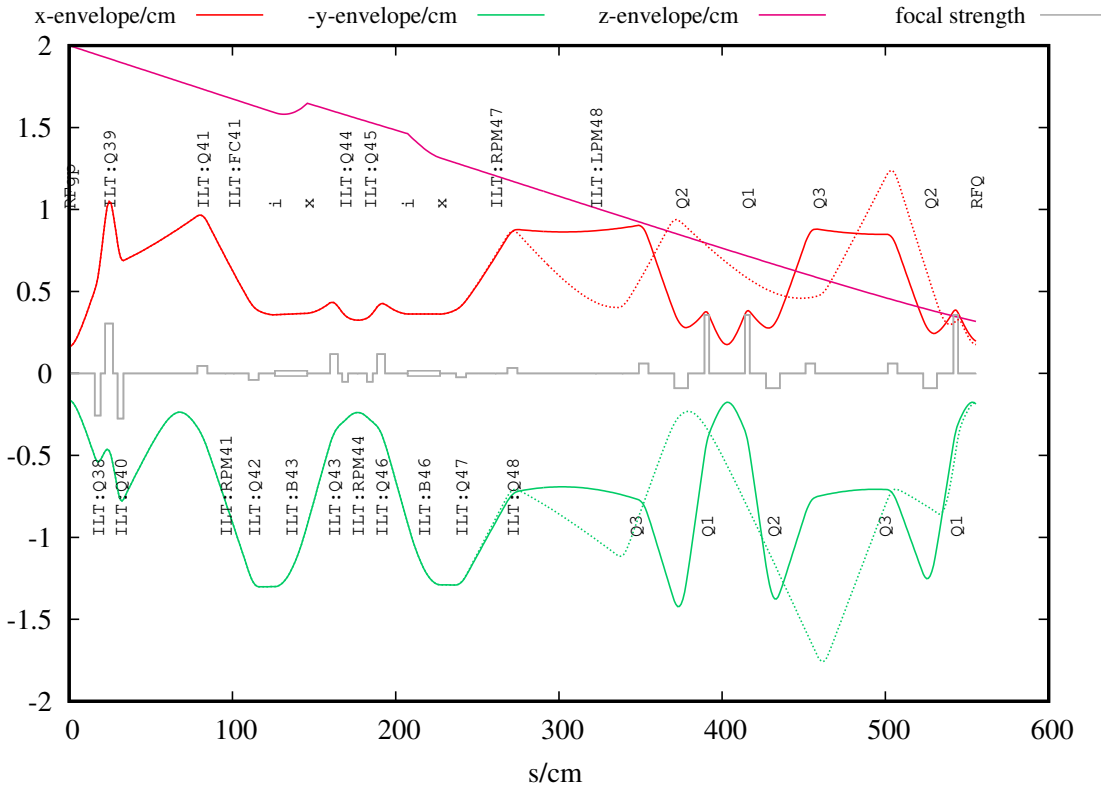

Figure 10: TRANSOPTR computed (x, y) envelopes showing a focus-to-focus, **with corrected Q3 positions**, starting at the ISAC prebuncher midpoint and terminating at RFQ injection. Quadrupole relative focal strengths are shown in grey. An emittance of 50μm is used.

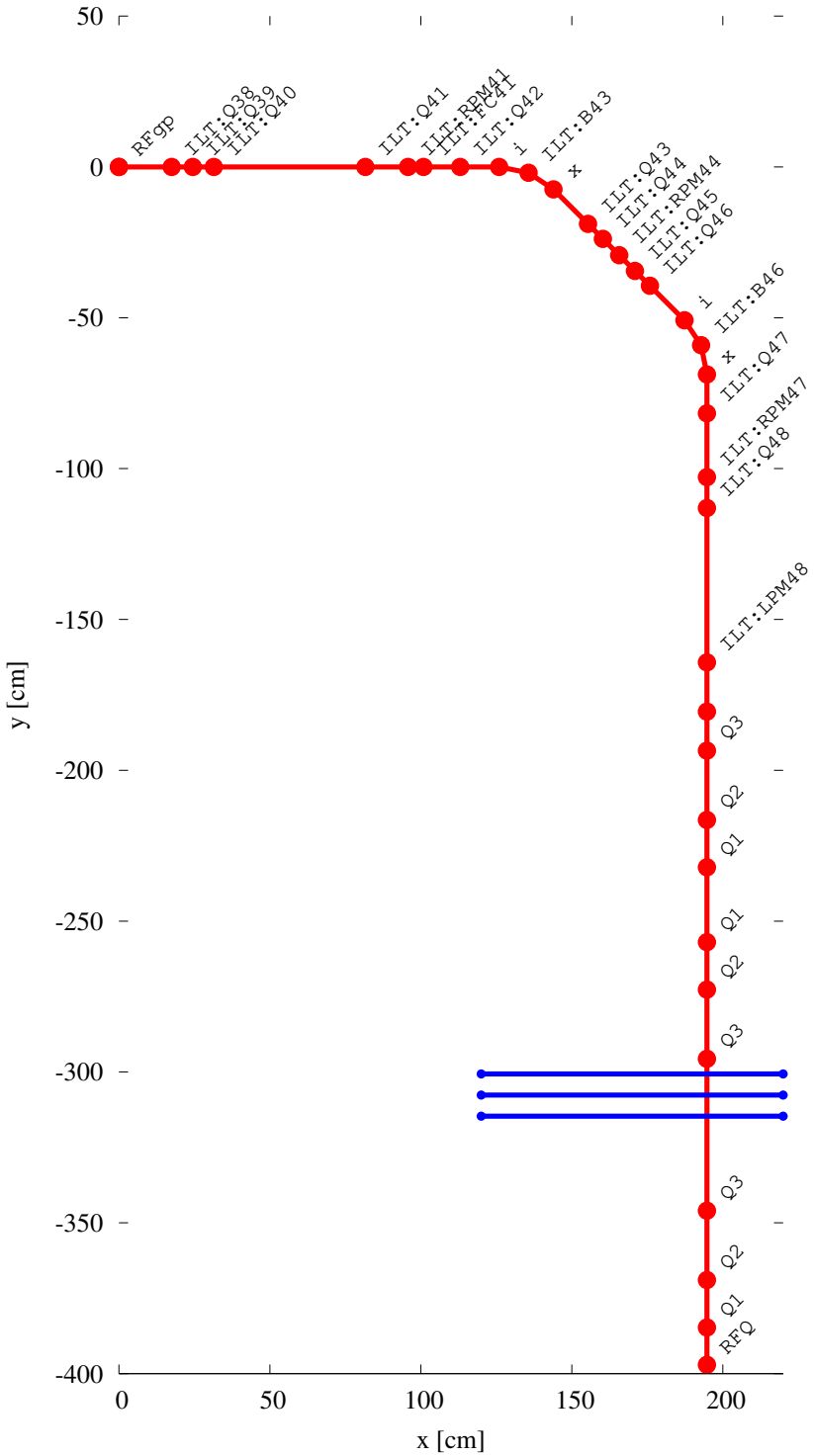

Figure 11: New ILT/IRA beamline layout, **with corrected Q3 positions**. Beam propagates clockwise from top left to bottom right. Blue horizontal lines show width of CANREB vacuum beamline at location of cross, shown in Figure 6.

The identified steerer locations in Fig. 12 are demonstrated in Fig. 13. This time, the reference particle is forward-propagated through the optics, again with the same tune. The effect of the selected steerers is demonstrated this time suing centroid errors of $(x, x') = (-y, y') = (2mm, 15\text{mrad})$ shown in Figure 13. The chosen locations enable a reduction of the off-axis error through the RF booster, in addition to the second and third periods of the new lattice. The RFQ injection error can also be minimized. Transverse intensity distribution imaging at two locations, both upstream and downstream of the booster, will enable comprehensive studies of the injected beam properties. A new fast Faraday cup device should be installed between the quadrupoles q2-q3 which follow the RF booster, with an available empty space of roughly 15 cm between devices. This will enable recording of the injected time-structure into the RFQ, enabling characterization of the prebuncher's time focus, even in cases where the RF booster is unused. For booster usage, the time-diagnostic will be essential for characterizing the longitudinal injection correction of the rf device.

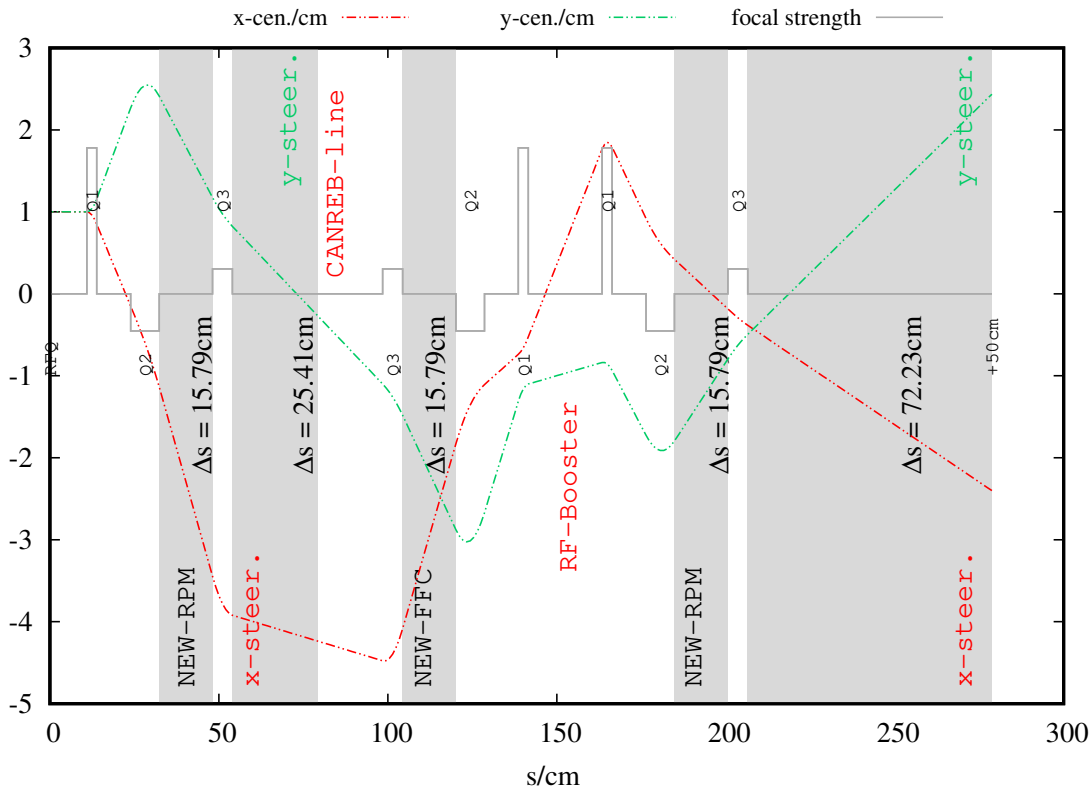

Figure 12: A reversed TRANSOPTR model of the new injection optics, showing reference particle centroids for (x, y), starting at RFQ entrance and ending into the ILT line. Beam has been started with a 1 cm offset in (x, y), but zero divergence. Shaded grey ares show possible locations for transverse steerers. For good effect, corrective steerers should be placed at locations where significant position-momentum correlations exist. Rough locations where this conditions exist and free space is available are labeled `x-steer.` and `y-steer.`

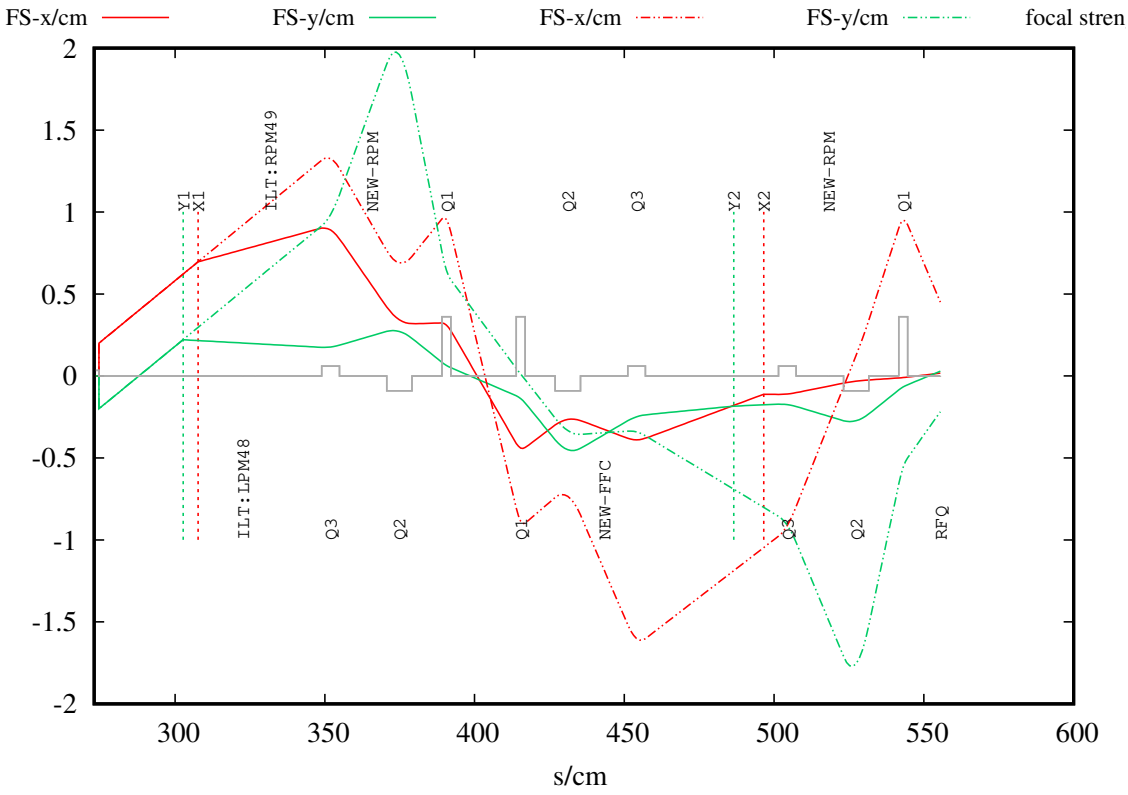

Figure 13: TRANSOPTR computed (x, y) Frenet-Serret (FS) centroids for (x, y) **with corrected Q3 positions**, starting 50cm upstream of the new injection optics. Steerer positions are shown as vertical dotted lines, and allow for the reduction of the centroid errors in both rf booster and RFQ injection. The uncorrected FS errors are shown as dotted lines, while the corrected centroids are solid.

5 Select `fort.label` Centerpoints For New Layout

[device]	s[cm]	ISAC-y[cm]	ISAC-x[cm]	
ISAC-PBN	0.000000	0.000000	0.000000	
ILT:Q38	17.467602	0.000000	17.467602	
ILT:Q39	24.452606	0.000000	24.452600	
ILT:Q40	31.437611	0.000000	31.437599	
ILT:Q41	81.635651	0.000000	81.635643	
ILT:RPM41	95.740494	0.000000	95.740555	
ILT:FC41	100.866058	0.000000	100.866142	
ILT:Q42	113.032532	0.000000	113.032639	
ILT:B43	135.925659	-1.933451	135.671310	
ILT:Q43	162.109680	-18.901300	155.373474	
ILT:Q44	169.094452	-23.840300	160.312500	
ILT:RPM44	176.736694	-29.244152	165.716354	
ILT:Q45	184.105957	-34.454967	170.927185	
ILT:Q46	191.090820	-39.394043	175.866257	
ILT:B46	217.275024	-59.096146	192.834076	
ILT:Q47	240.125153	-81.691742	194.767517	
ILT:RPM47	261.255066	-102.821686	194.767517	
ILT:Q48	271.522156	-113.088661	194.767517	
y-steer1	302.650452	-144.217651	194.767517	
x-steer1	307.650452	-149.217651	194.767517	
ILT:LPM48	322.650452	-164.217651	194.767517	
ILT:RPM49	331.749329	-173.316650	194.767517	
Q3	351.925781	-193.492950	194.767517	(eff.len.=5.8928cm, aper.-diam.=2.54cm)
NEW-RPM	365.662354	-207.229385	194.767517	
Q2	374.878906	-216.445755	194.767517	(eff.len.=8.4328cm, aper.-diam.=2.54cm)
Q1	390.608765	-232.175339	194.767517	(eff.len.=2.9465cm, aper.-diam.=2.54cm)
Q1	415.392822	-256.959351	194.767517	
Q2	431.122681	-272.689087	194.767517	
NEW-FFC	443.234009	-284.800476	194.767517	
Q3	454.075317	-295.641876	194.767517	
y-steer2	486.482483	-328.048248	194.767517	
x-steer2	496.482483	-338.048248	194.767517	
Q3	504.429016	-345.994690	194.767517	
NEW-RPM	518.165527	-359.731171	194.767517	
Q2	527.381836	-368.947601	194.767517	
Q1	543.111328	-384.677277	194.767517	
RFQ-start	555.502686	-397.069244	194.767517	

6 Select `fort.label` Centerpoints For Original Layout

[device]	s[cm]	ISAC-y[cm]	ISAC-x[cm]
RFgp	0.000000	0.000000	0.000000
ILT:Q38	17.467602	0.000000	17.467602
ILT:Q39	24.452599	0.000000	24.452600
ILT:Q40	31.437595	0.000000	31.437599
ILT:Q41	81.635635	0.000000	81.635643
ILT:RPM41	95.740479	0.000000	95.740555
ILT:FC41	100.866089	0.000000	100.866142
ILT:Q42	113.032608	0.000000	113.032639
ILT:B43	135.925781	-1.933451	135.671310
ILT:Q43	162.109833	-18.901300	155.373474
ILT:Q44	169.094604	-23.840300	160.312500
ILT:RPM44	176.736694	-29.244152	165.716354
ILT:Q45	184.105957	-34.454967	170.927185
ILT:Q46	191.090820	-39.394043	175.866257
ILT:B46	217.275024	-59.096146	192.834076
ILT:Q47	240.125153	-81.691742	194.767517
ILT:RPM47	261.255066	-102.821686	194.767517
ILT:Q48	271.522156	-113.088661	194.767517
ILT:LPM48	322.651062	-164.217499	194.767517
ILT:Q49	339.512817	-181.079300	194.767517
ILT:RPM49	353.613037	-195.179153	194.767517
ILT:FC49	358.240845	-199.807053	194.767517
ILT:Q50	370.910156	-212.476227	194.767517
ISAC1:RFB	382.509949	-224.076141	194.767517
IRA:Q1	461.897034	-303.463531	194.767517
IRA:RPM1	478.221375	-319.787781	194.767517
IRA:Q2	504.453064	-346.018829	194.767517
IRA:Q3	537.119751	-378.685913	194.767517
IRA:Q4	545.374390	-386.940918	194.767517
RFQINJECT END	555.500000	-397.066040	194.767517

7 Conclusion

This report has presented a first order optics model of a prospective new RFQ injection optics. The design accomodates the new RF booster cavity, by minimizing the transverse extent of the beam inside the rf structure's drift tubes. This is achieved by using a symmetric triplet assemlby which produces a waist-to-waist condition both at the booster's centrepoint and at ISAC-RFQ injection. Dimensions of this layout have been provided. This document is intended to serve as a basis for a final mechanical design, which will conform to the optics presented herein.

References

[1] Robert Laxdal, Zhengting Ang, Thomas Au, Spencer Kiy, Stephanie Rädel, Olivier Shelbaya, Vladimir Zvyagintsev, et al. A 3-gap booster cavity to match ion source potential to rfq acceptance. In *29th Linear Accelerator Conf.(LINAC'18), Beijing, China, 16-21 September 2018*, pages 196–199. JACOW Publishing, Geneva, Switzerland, 2019.

[2] L. Root. *Initial Operation of the RFQ Pre-buncher With a $^{14}N^{+1}$ Beam*. Technical Report TRI-DN-ISAC-00-05, TRIUMF, 1998.

[3] RL Poirier, P Bricault, K Fong, AK Mitra, HW Uzat, and Yu V Bylinsky. Rf systems of the triumf isac facility. In *Proceedings of the 1999 Particle Accelerator Conference (Cat. No. 99CH36366)*, volume 1, pages 450–452. IEEE, 1999.

[4] O Shelbaya, R Baartman, and O Kester. Fast radio frequency quadrupole envelope computation for model based beam tuning. *Physical Review Accelerators and Beams*, 22(11):114602, 2019.

[5] Olivier Shelbaya. ISAC-RFQ Parameter Documentation . Technical Report TRI-BN-22-07, TRIUMF, 2022.

[6] M Marchetto, J Aoki, K Langton, RE Laxdal, W Rawnsley, JE Richards, et al. The ISAC-II current monitor system. *LINAC10, Tsukuba*, 2010.